Available online at www.sciencedirect.com
SCIENCE DIRECT
Journal of Photochemistry and Photobiology A: Chemistry 179 (2006) 105–114
Journal of Photochemistry and Photobiology A:Chemistry
www.elsevier.com/locate/jphotochem

Visible-light induced photocatalytic activity of $TiO_{2-x}A_y$ (A = N, S) prepared by precipitation route

S. Yin *, K. Ihara, Y. Aita, M. Komatsu, T. Sato

Institute of Multidisciplinary Research for Advanced Materials, Tohoku University, Sendai 980-8577, Japan

Received 5 January 2005; received in revised form 5 July 2005; accepted 2 August 2005
Available online 6 September 2005

Abstract

Nitrogen doped or nitrogen/sulfur co-doped titania photocatalyst $TiO_{2-x}A_y$ (A = N, S) which can be excited by visible light were prepared by mixing aqueous $TiCl_3$ solutions with various nitrogen sources such as hydroxylamine (NH_2OH), hexamethylenetetramine (HMT, $C_6H_{12}N_4$), urea ($(NH_2)_2CO$) and thiourea ($(NH_2)_2CS$) followed by hydrothermal treatment at 190 °C. The titania powders prepared using hydroxylamine consisted of rutile crystals with non-homogeneous size distribution. The nitrogen doped titania powders prepared using hexamethylenetetramine consisted of mainly mono-size spherical brookite crystals, whereas those using urea and thiourea consisted of belt-like rutile particles. The $TiO_{2-x}A_y$ (A = N, S) powders showed excellent visible-light absorption and photocatalytic ability for the oxidative destruction of nitrogen monoxide under irradiation of visible light. The effect of reaction solvents on the phase composition, specific surface area and photocatalytic activity was also characterized.

Keywords: Precipitation route; Anion dope; TiO_2; Visible-light induced; Photocatalyst

1. Introduction

Titania is the most effective photocatalyst and widely applied in purification of air and water, deodorization, antibacterial and self-cleaning coating and other environmental applications. However, titania can only be encouraged by UV light because of its large band gap value of ca. 3 eV. In order to utilize the solar energy efficiently, it is necessary to develop a visible-light reactive photocatalyst. In 2001, Asahi et al. [1,2] reported that nitrogen doped titanium oxide with high visible-light photocatalytic activities could be prepared by sputtering TiO_2 in an N_2 (40%)/Ar gas mixture followed by annealing in N_2 gas at 550 °C or by treating anatase TiO_2 powder in the NH_3 (67%)/Ar atmosphere at 600 °C. They also theoretically calculated the band structure of some anion doped titania by the first-principles calculations and pointed out that nitrogen doping leads to narrowing of band gap by mixing the N2p and O2p state and consequently induces the visible-light responsive photocatalytic activity. It was also forecasted that other kind of anions such as C, S and F would result in the similar effect to nitrogen. Since then, many researchers paid their much attention on anion doped photocatalysts [3–8]. However, most methods are high temperature processes, using expensive precursors or preparation instruments. In our previous research, it was found that nitrogen, fluorine or sulfur doped photocatalyst with high visible-light induced photocatalytic activity could be prepared by a low-temperature mechanochemical doping process [9–12]. However, anion doped titania in only rutile structure can be prepared by this process. In order to realize the phase-compositional and morphological control of anion doped photocatalysts, a novel solution process is described in this paper, using various precipitation sources. The effects of reaction conditions such as pH and type of solvents on phase composition, particle size, microstructure, specific surface area and photocatalytic activity were investigated in detail. In addition, the photocatalytic activity for the oxidative destruction of nitrogen monoxide under irradiation of visible light was investigated.

* Corresponding author. Tel.: +81 22 217 5598; fax: +81 22 217 5598.
E-mail address: shuyin@tagen.tohoku.ac.jp (S. Yin).

1010-6030/$ – see front matter © 2005 Elsevier B.V. All rights reserved.
doi:10.1016/j.jphotochem.2005.08.001

2. Experimental

Nitrogen doped or nitrogen/sulfur co-doped titania photocatalyst $TiO_{2-x}A_y$ (A = N, S) were prepared by mixing aqueous $TiCl_3$ solutions with various nitrogen sources such as hydroxylamine (NH_2OH), hexamethylenetetramine (HMT, $C_6H_{12}N_4$), urea ($(NH_2)_2CO$)) and thiourea ($(NH_2)_2CS$)) (Kanto Chem. Co. Inc., Japan) followed by hydrothermal treatment at 190 °C. After adding 2 g of nitrogen sources and 21.5 cm^3 of 20 wt.% $TiCl_3$ solution into 25 cm^3 of distilled water or alcohols, the mixed solution was placed into a SUS 314 stainless steel autoclave attached with a Teflon tube of internal volume of 200 cm^3. After that the chamber of autoclave was flushed by nitrogen gas three times. The autoclave was heated and kept at 90 °C for 1 h, then heated at 190 °C for 2 h. The final pH value of the urea solution was controlled to 2, 7 and 9 by using 2, 6 and 10 g of urea. The powder product was separated by centrifugation, washed with distilled water and acetone three times, respectively, then vacuum dried at 80 °C overnight.

The phase composition of the products was determined by X-ray diffraction analysis (XRD, Shimadzu XD-D1) using graphite-monochromized Cu Kα radiation. The specific surface areas were determined by the amount of nitrogen adsorption at 77 K (BET, Quantachrome NOVA 1000-TS). Microstructures were observed by a transmission electron micrograph (TEM, JEOL JEM-2010). The absorption edges and band gap energies of the products were determined from the onsets of diffuse reflectance spectra of the samples measured using an UV–vis spectrophotometer (Shimadzu UV-2000). The spectra of the light sources were measured by a multichannel spectrophotometer (JASCO, MD-100). The light intensity on the surface of photocatalyst was measured by a light meter (LI-COR, LI-189, USA) with a quantum type sensor. The binding energy of N1s and S2p was measured using Ar etching technique by an X-ray electron spectrometer (Pekin-Elmer PHI5600). The doping amount of nitrogen and sulfur were determined by the integrated intensity ratio of the peaks around 396 eV (Ti–N bonding) or 162 eV (Ti–S bonding) to the total integrated intensity of the O1s, Ti2p, N1s and S2p peaks. The photocatalytic activity for nitrogen monoxide destruction was determined by measuring the concentration of NO gas at the outlet of the reactor (373 cm^3 of internal volume) during the photo-irradiation of a constant flow (200 cm^3/min) of a mixture containing 1 ppm NO—50 vol.% air (balance N_2) [13]. The photocatalytic sample was placed in a hollow of 20 mm length × 16 mm width × 0.5 mm depth on a glass holder plate and set in the bottom center of the reactor. A 450 W high-pressure mercury arc was used as the light source. The wavelength was controlled by selecting filters, i.e., Pyrex glass for λ > 290 nm, Kenko L41 Super Pro (W) filter >400 nm and Fuji triacetyl cellulose filter >510 nm. The concentration of NO was determined using a NO_x analyzer (Yanaco, ECL-88A). For comparison, a photocatalytic reaction was also carried out using commercial titania (Degussa P25).

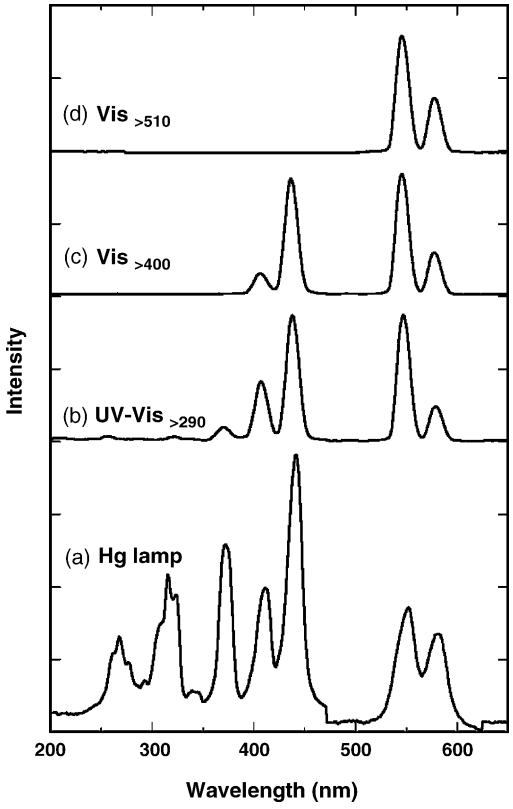

Fig. 1. Wavelength distribution of the light irradiated from a 450 W high-pressure mercury lamp (a) without filter, (b) light (a) filtered by Pyrex glass jacket (UV–$vis_{>290}$), (c) light (b) filtered by a 400 nm cut-off filter ($Vis_{>400}$) and (d) light (c) filtered by a 510 nm cut-off filter ($Vis_{>510}$).

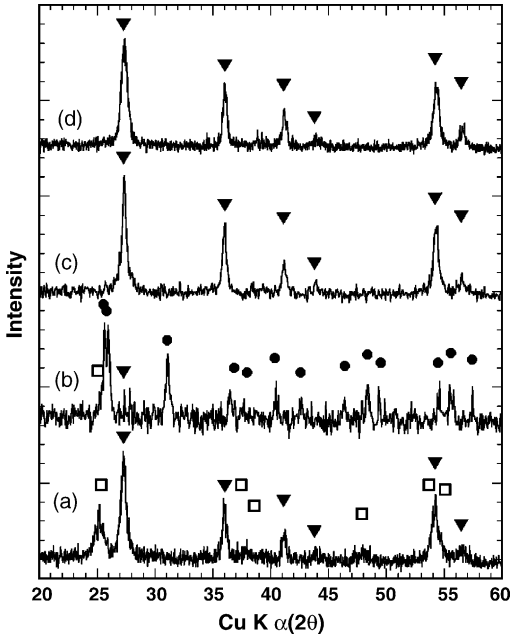

Fig. 2. XRD patterns of the titania powders prepared at 190 °C for 2 h using (a) NH_2OH, (b) $C_6H_{12}N_4$, (c) $(NH_2)_2CO$ and (d) $(NH_2)_2CS$ as precipitation reagents. (□) Anatase; (▼) rutile; (●) brookite.

3. Results and discussion

3.1. Characterization of $TiO_{2-x}A_y$ (A = N, S) prepared by using various precipitation sources

The photocatalytic activities of the prepared samples were investigated under the irradiating lights with various wavelengths. Fig. 1 shows the spectra of the light source filtered by different filters. It is seen that the light of the wavelength less than 290, 400 and 510 nm could be filtered out using a Pyrex glass jacket, 400 nm cut-off filter and 510 nm cut-off filter, respectively. The light intensity of $\lambda > 290$ nm (UV–vis$_{>290}$), $\lambda > 400$ nm (Vis$_{>400}$) and $\lambda > 510$ nm (Vis$_{>510}$) on the surface of photocatalyst were identified as 352, 337 and 243 μmol m^{-2} s^{-1}, respectively.

It is known that urea, hexamethylenetetramine and thiourea decompose at high temperatures [14–17]. The

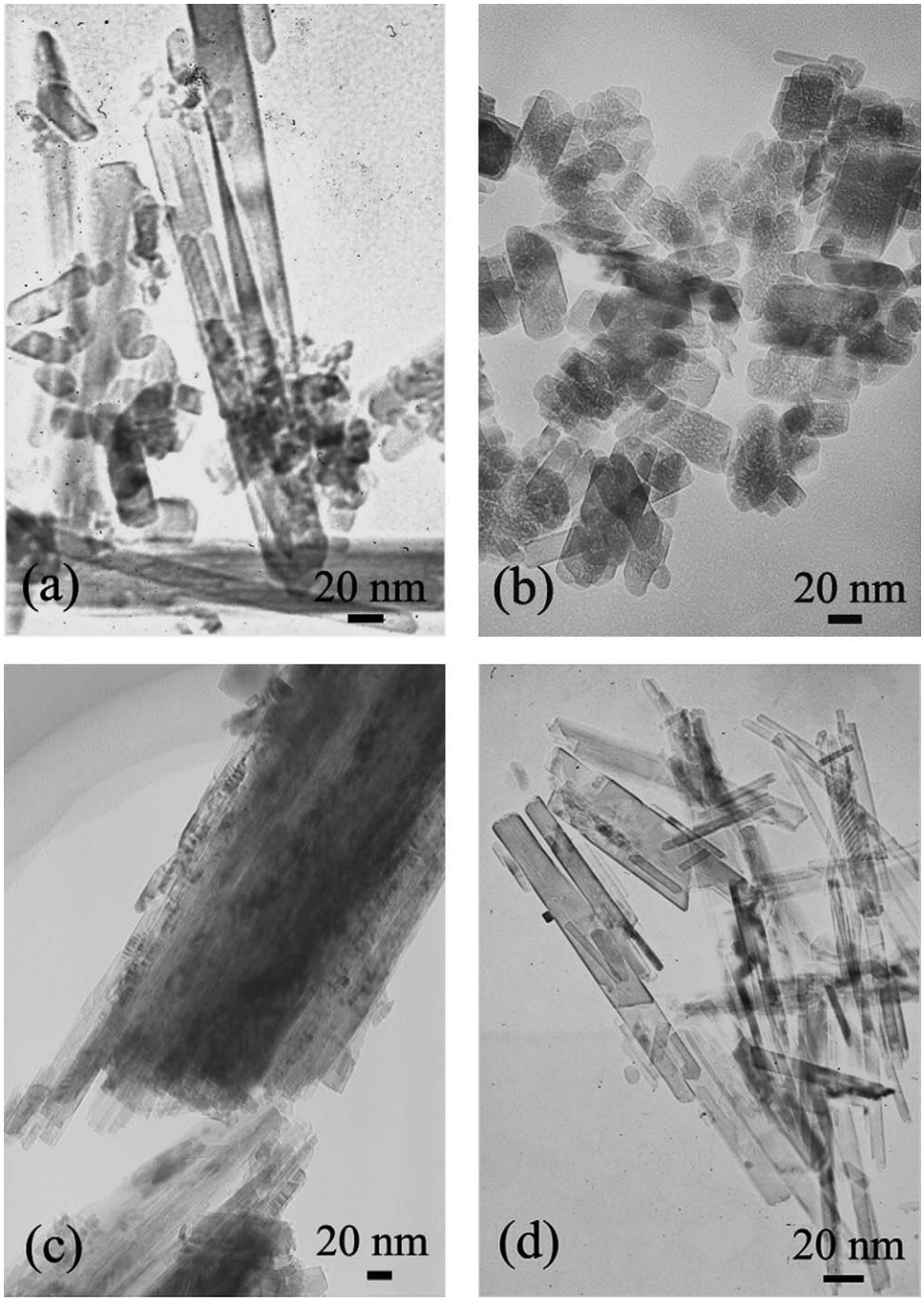

Fig. 3. TEM photographs of the titania powders prepared at 190 °C for 2 h using (a) NH_2OH, (b) $C_6H_{12}N_4$, (c) $(NH_2)_2CO$ and (d) $(NH_2)_2CS$ as precipitation reagents.

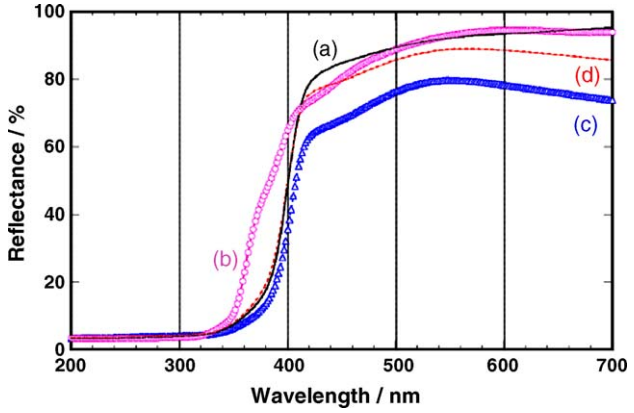

Fig. 4. Diffuse reflectance spectra of the titania powders prepared at 190 °C for 2 h using (a) NH_2OH, (b) $C_6H_{12}N_4$, (c) $(NH_2)_2CO$ and (d) $(NH_2)_2CS$ as precipitation reagents.

decomposition products react with $TiCl_3$ to form $TiO_{2-x}A_y$ (A = N, S):

$$TiCl_3 \xrightarrow[NH_2OH;\, C_6H_{12}N_4;\, (NH_2)_2CO;\, (NH_2)_2CS]{90\,^\circ C} TiO_{2-x}A_y \cdot nH_2O$$

$$\xrightarrow[\text{in autoclave}]{190\,^\circ C} TiO_{2-x}A_y\,(A = N,\ S) \qquad (1)$$

Fig. 2 shows the XRD patterns of the titania powders prepared at 190 °C for 2 h using hydroxylamine, hexamethylenetetramine, urea and thiourea as precipitation reagents. The final pH value was about 2. It was found that the phase composition is strongly related to the kind of precipitate reagents. A mixture of anatase and rutile was formed by using hydroxylamine. A brookite phase consisted of a little amount of anatase and rutile could be formed by hexamethylenetetramine, while single phase of rutile was produced by urea and thiourea.

Fig. 3 shows TEM photographs of the $TiO_{2-x}A_y$ (A = N, S) powders prepared at 190 °C for 2 h. It was obvious that short rod-like particles were formed in $TiCl_3$–hexamethylenetetramine solution (Fig. 3(b)), while rod-like structures were obtained in $TiCl_3$–urea/thiourea solution. On the other hand, the powders prepared in hydroxylamine solution consisted of a mixture of rod-like and spherical powders (Fig. 3(a)). Compared with the XRD pattern of Fig. 1, it might be estimated that the rod-like powders consisted of rutile phase, and the spherical particles related to the anatase phase.

Fig. 4 shows the diffuse reflectance spectra of the prepared $TiO_{2-x}A_y$ (A = N, S) powders. It is obvious that all the $TiO_{2-x}A_y$ powders prepared in hexamethylenetetramine, urea and thiourea showed visible-light absorption in the range of 400–550 nm and possessed two absorption edges around 410 and 530 nm, indicating the formation of N/S–Ti bonding in the $TiO_{2-x}A_y$ (Fig. 4(b–d))). The first absorption edge around 410 nm was related to the original structure of titania. The second absorption edge should be related to the newly formed N1s or S2p orbits caused by the nitrogen and/or sulfur doping in the molecular structure. It was reported that sulfur could be doped in titania molecular by mixing titanium isopropoxide with thiourea in ethanol followed by evaporation and calcination in air [18]. In our previous paper, it was also confirmed that N–Ti bonding could be formed by a hydrothermal process in hexamethylenetetramine aqueous solution system [19]. The difference on the spectra around 370–420 nm was caused by the different phase composition of $TiO_{2-x}A_y$. In the case of mixing $TiCl_3$ solution with hydroxylamine, the precipitation reaction occurred rapidly to produce violet $Ti(OH)_3$ precipitate at first, then the precipitate was oxidized to white $Ti(OH)_4$ immediately at room temperature before crystallization in autoclave. Because the violet Ti^{3+} precipitate is unstable in the air atmosphere, the powders prepared in $TiCl_3$–hydroxylamine solution showed white color and only one absorption edge, indicating no nitrogen doping existed in the lattice of titania (Fig. 4(a)). On the other hand, the powders prepared in hexamethylenetetramine, urea or thiourea showed beige, weak violet and gray color, respectively. In the case of mixing $TiCl_3$ solution with these three kinds of precipitants, no precipitate was obtained at low temperature range because these precipitants are stable in aqueous solution below 70 °C. As a result, the precipitation process proceeded at higher temperature in nitrogen gas flashed autoclave, together with the followed hydrothermal crystallization process. The final powders consisted of different small amount of low-valence compound TiO_{2-x} in the titania, which led to the decrease of reflectance between 500 and 700 nm. It was found that the violet color caused by the TiO_{2-x} was stable in air atmosphere at room temperature. Similarly, it was also reported that the low-valence compound TiO_{2-x} showed a wide and strong absorption in the wavelength range more than 500 nm [20].

Fig. 5 shows the photocatalytic activity and the quantum efficiency of the powders under irradiation of light with various wavelength ranges. In the present study, the photocatalytic characterization system was similar to that of the Japanese Industrial Standard, which was established at the beginning of 2004 [21], although some detail conditions were different. In this JIS standard, it is recommended that the photocatalytic activity of photocatalyst should be characterized by measuring the decrease in the concentration of NO at the outlet of a continuous reactor. A 1 ppm of NO gas with a flow rate of 3.0 dm^3/min is introduced to a reactor (area of photocatalyst: 100 mm × 50 mm) then irradiated by a lamp with light wavelength of 300–400 nm. It is accepted that electron/hole pairs are formed by the photo-excitation of titania. In the presence of oxygen, the electrons in the conduction band are immediately trapped by the molecular oxygen to form $^\bullet O_2^-$, which can then generate active $^\bullet$OOH radicals [22,23]. It is known that the nitrogen monoxide reacts with these reactive oxygen radicals, molecular oxygen and very small amount of water in air to produce mainly HNO_2 or HNO_3, and 20% of nitrogen monoxide was decomposed to nitrogen and oxygen directly [24]. It is obvious that the powders prepared in hexamethylenetetramine,

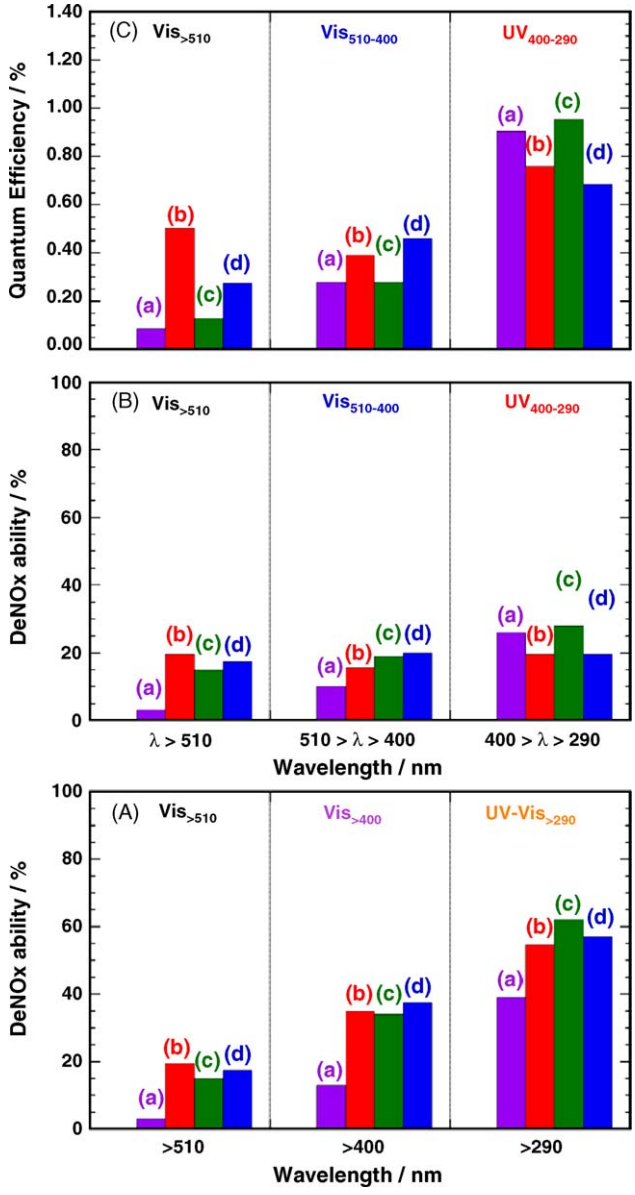

Fig. 5. The photocatalytic activity and the quantum efficiency of the samples prepared at 190 °C for 2 h using (a) NH_2OH, (b) $C_6H_{12}N_4$, (c) $(NH_2)_2CO$ and (d) $(NH_2)_2CS$ as precipitation reagents. The data were treated against various wavelength ranges.

urea or thiourea possessed higher visible light ($Vis_{>510}$ and $Vis_{>400}$) and UV–vis light ($UV–vis_{>290}$) responsive activity than that prepared in hydroxylamine (Fig. 5(A)). The NO concentration at the outlet of the reactor decreased under photo-irradiation and returned to its initial level of 1 ppm within 10 min when the light was turned off, indicating that light energy is necessary for the oxidation of nitrogen monoxide. As shown in Fig. 1, the light $Vis_{>400}$ consisted the wavelength of 400–500 nm and >510 nm, and the light $UV–vis_{>290}$ consisted all the light wavelength of 290–400, 400–500 and >510 nm. In order to characterize the quantum efficiency (QE), the data of Fig. 5(A) were treated against different wavelength range (Fig. 5(B and C)). Based on the light intensity result of Fig. 1, it could be calculated that the light intensity of 290 nm < λ < 400 nm ($UV_{400–290}$), 400 nm < λ < 510 nm ($Vis_{510–400}$) and λ > 510 nm ($Vis_{>510}$) were 15, 94 and 243 μmol m^{-2} s^{-1}, respectively. Take the consideration of the $deNO_x$ ability and average absorption ratio in their light range (Fig. 4), the QE can be calculated against wavelength according to the following equation:

$$QE_\lambda = \frac{F_{NO} \cdot \alpha_\lambda}{P_\lambda \cdot S \cdot A_\lambda} \times 100\% \quad (2)$$

where QE_λ(%) is the quantum efficiency under irradiation of light with various wavelength range, i.e., 290 nm < λ < 400 nm ($UV_{400–290}$), 400 nm < λ < 510 nm ($Vis_{510–400}$) and λ > 510 nm ($Vis_{>510}$), respectively; F (μmol s^{-1}) the flow quantity of NO molecules in the reaction gas; α_λ (%) the $deNO_x$ ability of the photocatalyst; P_λ (μmol m^{-2} s^{-1}) the light intensity on the surface of the sample; S (m^2) the surface area of the samples (20 mm × 16 mm); A_λ (%) is the average light absorption ratio of samples in various wavelength range (see Fig. 4). It is obvious that the sample (c) prepared in urea possessed higher $QE_{400–290}$ (0.955%) than others in $UV_{400–290}$ range; while the sample (b) prepared in hexamethylenetetramine showed the highest $QE_{>510}$ (0.504%) in $Vis_{>510}$ range. In all the cases, the $QE_{400–290}$ irradiated with UV light (290 nm < λ < 400 nm) was higher than that of $QE_{510–400}$ or $QE_{>510}$ with visible-light irradiation.

Table 1 summarizes the physical properties such as phase composition, specific surface area and photocatalytic activity of the prepared powders. The microstructure and specific surface area of titania powders greatly changed depending on the precipitation reagent and reaction conditions. Nitrogen doped

Table 1
Physical properties and photocatalytic ability for the destruction of nitrogen monoxide under irradiation of different wavelength light

Precipitation reagent[a]	Main phase composition	S_{BET} (m^2 g^{-1})	NO destruction ability (%)		
			>510 nm	>400 nm	>290 nm
NH_2OH	Rutile + anatase	84.6	4.0	10.0	35.0
HMT	Brookite	41.8	12.6	33.7	52.6
Urea	Rutile	25.8	12.0	31.0	59.0
Thiourea	Ruile	31.5	15.8	32.6	55.8

[a] Followed by hydrothermal treatment at 190 °C for 2 h.

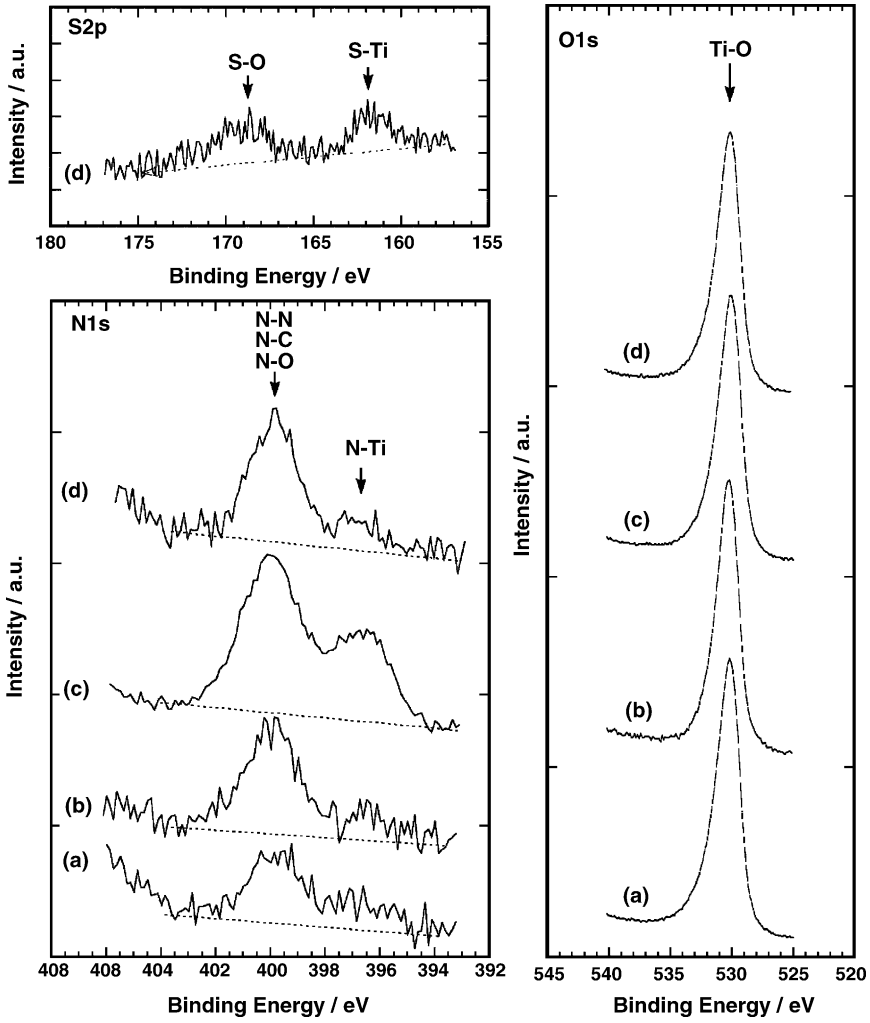

Fig. 6. N1s, O1s and S2p XPS spectra of the titania prepared using (a) NH_2OH, (b) $C_6H_{12}N_4$, (c) $(NH_2)_2CO$ and (d) $(NH_2)_2CS$ as precipitation reagents. The measurement was carried out after Ar^+ ion sputtering for 3 min.

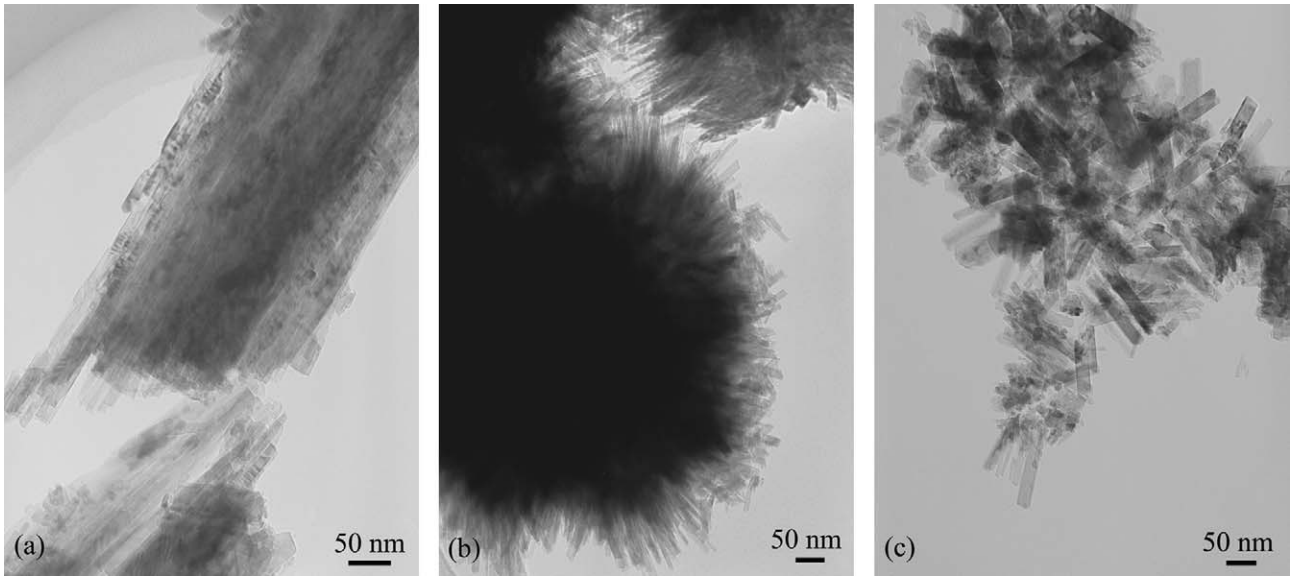

Fig. 7. TEM photographs of the titania prepared by heat treatment of $TiCl_3$–urea solution at 190 °C and (a) pH 2, (b) pH 7, (c) pH 9 for 2 h.

brookite/rutile titania and nitrogen/sulfur co-doped rutile titania nanocrystals with excellent visible-light induced photocatalytic activity were successfully synthesized. In the case of using hydroxylamine as a precipitation reagent, amorphous titania precipitate was formed immediately in the solution before hydrothermal treatment, the products after hydrothermal treatment in solution consisted of the mixture of large and small particles with non-homogeneous size distribution. On the other hand, in the case of using other three kinds of nitrogen sources, the precipitation reaction and crystallization were realized simultaneously during hydrothermal treatment, resulting the mono-sized distribution of products. In addition, the powders prepared in $TiCl_3$–hydroxylamine solution showed lower nitrogen content and lower photocatalytic activity under both visible and UV light irradiation.

Fig. 6 shows the N1s, O1s and S2p spectra of the prepared $TiO_{2-x}A_y$ powders. It was found that the N1s peak around 400 eV but without the peak around 396 eV could be observed for all as-prepared $TiO_{2-x}A_y$ samples before Ar ion sputtering treatment because the adsorbed large amount of ammonia and other nitrogen compound on the surface (400 eV) hid the existence of Ti–N binding (396 eV). The peak intensity around 400 eV decreased and that around 396 eV increased step-by-step with increasing Ar^+ ion sputtering treatment time until 3 min. However, the peak intensity around 396 eV came to a steady intensity level for more than 3 min sputtering treatment. The binding energy around 396 eV that related to the existence of N–Ti could be confirmed in the $TiO_{2-x}A_y$ samples prepared by using various nitrogen reagents, indicating that Ti–N binding was actually formed in the lattice of the titania crystal during the hydrothermal treatment. It is known that the peak around 400 eV is related to the N–N [1,2]. It was obvious that the intensity of the Ti–N peak of the sample prepared in hydroxylamine (Fig. 6(a)) was weaker than those prepared by using hexamethylenetetramine (Fig. 6(b)), urea (Fig. 6(c)) and thiourea (Fig. 6(d)) as precipitant. It is know that binding energy around 162 eV is related to the existence of S–Ti, and that around 168 eV is related to the S–O bonding [12]. The S–Ti binding could be observed in the powders prepared using $(NH_2)_2CS$ as precipitant, indicating that N and S were co-doped in the lattice of titania (Fig. 6(d)). On the other hand, no obvious difference on the O1s peak could be found for the different titania powders. According to the integrated intensity of the peaks around 396 eV, it was found that about 0.29, 0.54, 2.24 and 0.49% N–0.08% S were really incorporated into the TiO_2 lattices (peak at 396 eV) of the samples (a–d), respectively. Compared with the DRS spectra (Fig. 4), it was found that some disagreement between XPS and DRS spectra of the samples (a–d) existed. It is worthy of notice that not only nitrogen doping, but also phase composition and the existence of Ti^{3+} affect the absorption of the powders in visible-light range, i.e., affect the shapes of the DRS spectra. Taking every factor into consideration, it is easy to understand the difference between them, although the detail is not clarified completely.

3.2. Thermal stability of $TiO_{2-x}N_y$

As mentioned above, $TiO_{2-x}A_y$ powders could be successfully prepared by using various precipitation reagents. The $TiO_{2-x}N_y$ powders prepared in $TiCl_3$–urea solution possessed higher nitrogen doped content and excellent photocatalytic activity. In addition, because no dangerous gas such as HCHO was produced, it was easy to be operated than other solution system. So the $TiCl_3$–urea solution system was focused on the following research. It was found that the powders prepared at pH 2 in $TiCl_3$–urea aqueous solutions consisted of single phase rutile, while those at pH 7 and 9 were an anatase and rutile mixture. It seemed that phase transformation from anatase to rutile was promoted by decreasing pH, indicating the existence of NH_3 delayed the anatase to rutile phase transformation. The TEM photographs of the prepared powders are shown in Fig. 7. The powders obtained at pH 7 showed fine fibrous structure and high specific surface area of 108 $m^2\ g^{-1}$, which is two to four times higher than those

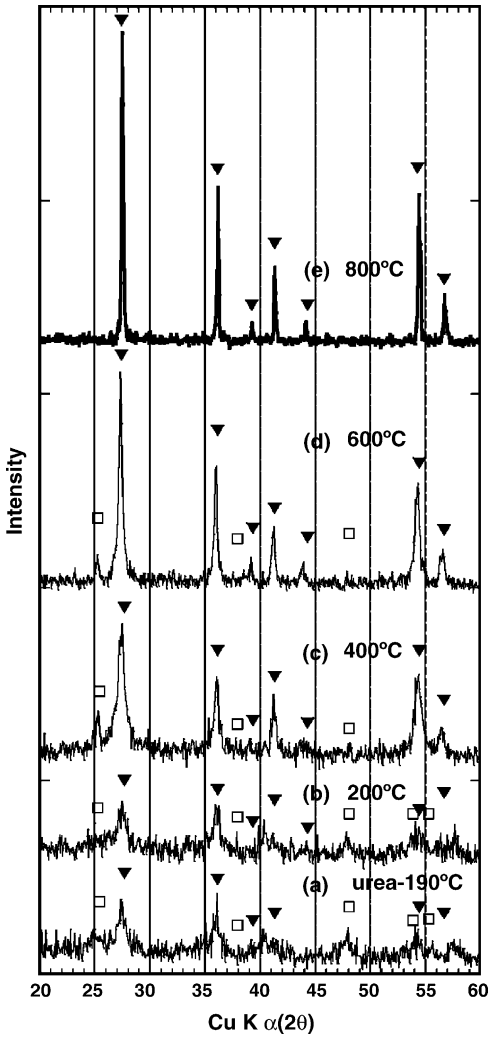

Fig. 8. XRD patterns of the titania powders prepared by (a) heat treatment of $TiCl_3$–urea solution at 190 °C and pH 7, followed by calcination in air at (b) 200 °C, (c) 400 °C, (d) 600 °C and (e) 800 °C. (□) Anatase; (▼) rutile.

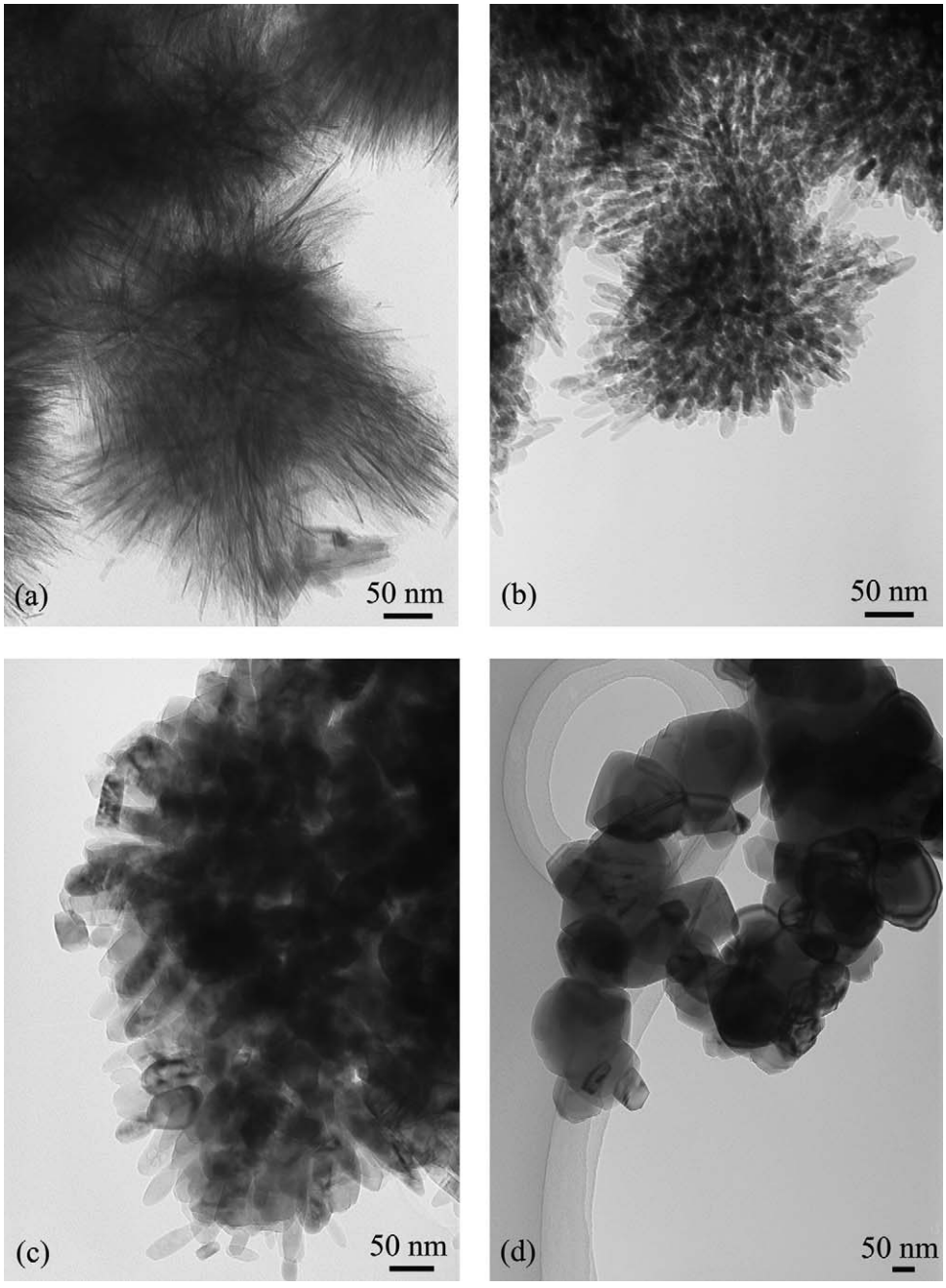

Fig. 9. TEM photographs of the titania powders prepared by heat treatment of $TiCl_3$–urea solution at 190 °C and pH 7, followed by calcination in air at (a) 200 °C, (b) 400 °C, (c) 600 °C and (d) 800 °C.

prepared at pH 2 (25.8 $m^2\,g^{-1}$) and pH 9 (61.4 $m^2\,g^{-1}$). The thermal stability of phase composition of the powders with high specific surface area was characterized. Fig. 8 shows the XRD pattern of the powders calcined in air at various temperatures. At 400 °C, the crystallinity increased a lot, above 800 °C, anatase transformed to rutile and the specific surface area greatly decreased as 3.4 $m^2\,g^{-1}$.

Fig. 9 shows TEM photographs of the titania powders calcined in air at different temperatures. It could be seen that the fine fibrous particles grew to large rod-like particles after high temperature calcination.

Fig. 10 shows the diffuse reflectance spectra of titania powders calcined in air at different temperatures. It was found that the titania powders prepared at pH 7 (Fig. 10(a)) showed deeper violet color and lower reflectance between 400 and 700 nm than those prepared at pH 2 (Fig. 4(c)), indicating more TiO_{2-x} existed in the prepared titania. After calcination in air at 200 and 400 °C, the color of titania changed to gray and bright yellow, indicating the decrease of TiO_{2-x} in the crystalline lattice. As a result, the reflectance between 500 and 700 nm related to the TiO_{2-x} increased, and the samples showed two absorption edges around 400 and 520–540 nm.

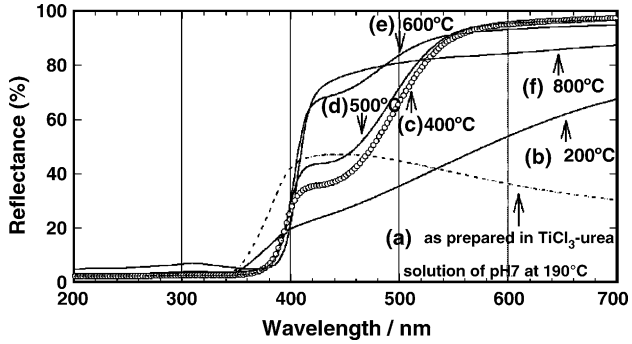

Fig. 10. Diffuse reflectance spectra of titania powders prepared by (a) heat treatment of $TiCl_3$–urea solution at 190 °C and pH 7 followed by calcination in air at (b) 200 °C, (c) 400 °C, (d) 500 °C, (e) 600 °C and (f) 800 °C.

The two-step absorption was stable until 600 °C. After calcination at 800 °C, only one absorption edge could be observed.

3.3. Characterization of $TiO_{2-x}N_y$ prepared from urea–alcohol solvents

Instead of aqueous solution, several kinds of alcohol such as methanol, ethanol, 1-propanol and 1-butanol were added in the solution. It was accepted that crystal growth in the solution greatly effected by the dielectric constant of the solution [23,25–27]. In this study, the effect of solvents on the phase composition, specific surface area and photocatalytic activity was investigated. Table 2 summarizes the reaction conditions including kind of solvent, final pH value of treatment and their affect on the physical properties of the products. Although five kinds of solvents were applied at different pH values, anatase phase formed in only methanol solution at pH 9.

It was found that single phase anatase could be obtained in the $TiCl_3$–urea methanol solution at pH 9, while a mixture

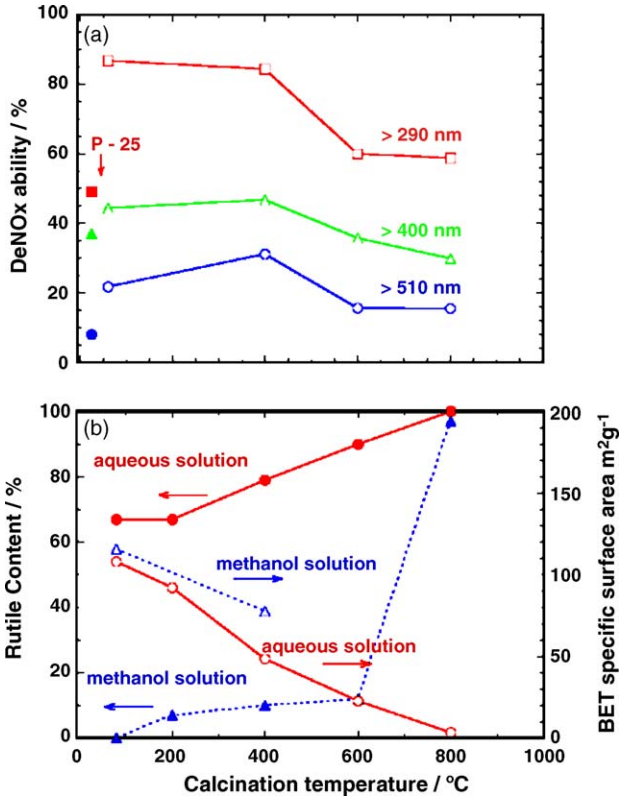

Fig. 11. The effect of calcination temperature on (a) photocatalytic activity (□, λ > 290; △, λ > 400 and ◯, λ > 500 nm), (b) the rutile phase fraction (solid marks), BET specific surface area (white marks) of $TiO_{2-x}N_y$ powders prepared by heat treatment in $TiCl_3$–urea aqueous solution (solid line) at pH 7 and $TiCl_3$–urea methanol solution (dotted line) at pH 9. The solid marks (■, ▲, ●) showed the photocatalytic activities of standard commercial powder Degussa P25.

Table 2
Effect of treatment solvents on the physical properties of nitrogen doped titania

Treatment solvent	Final pH	Phase composition[a]	S_{BET} ($m^2\ g^{-1}$)	Photocatalytic activity (%)		
				>510 nm	>400 nm	>290 nm
As received P25	–	A > R	47.3	8	37	49
Aqueous solution	1	R	25.2	12.0	31.0	59.0
	7	R + A	108.1	10.5	30.5	62.1
	9	R + A	61.4	10.6	35.8	52.9
Methanol aqueous solution	1	R + B	25.3	25.3	41.1	82.1
	7	A + R	101.9	11.1	38.9	82.2
	9	A	67.5	21.1	44.4	86.7
Ethanol aqueous solution	1	R	36.1	14.1	35.6	73.7
	7	A > R	64.0	15.0	35.0	74.0
	9	A > R	52.8	13.3	42.9	76.5
1-Propanol aqueous solution	1	R	17.4	8.7	26.1	71.7
	7	R > A	87.1	11.0	33.0	71.4
	9	R > A	33.1	12.0	33.7	73.9
1-Butanol aqueous solution	1	R	15.6	3.5	18.1	40.6
	7	R	43.8	4.3	21.5	52.6
	9	R	33.8	14.7	31.6	60.0

[a] A, Anatase; B, brookite; R, rutile.

of rutile and brookite was formed at pH 2. Other solvents resulted the formation of anatase and rutile mixture. Low pH values prefer to produce rutile phase. The powders consisted of single phase anatase or mixture of rutile and brookite prepared in methanol solution showed excellent photocatalytic activity under both visible and UV light irradiation.

Fig. 11 shows the calcination temperature dependence on BET specific surface area, phase composition and photocatalytic activity of the $TiO_{2-x}N_y$ powders prepared by $TiCl_3$–urea aqueous or methanol solutions. With increasing calcination temperature, the anatase fraction decreased and rutile fraction increased. The BET specific surface area decreased also. Usually, the photocatalytic activity strongly related with the specific surface area [23,25]. However, although the specific surface area decreased in about half after calcination at 400 °C, the photocatalytic activity did not decrease. This might be due to the removal of the absorbed by-products in the samples and the increase in crystallinity by calcination. The most excellent photocatalytic activity under visible light (>510 nm) was obtained from $TiCl_3$–urea methanol solution, continuously destructing nearly 21–25% of nitrogen monoxide (see Table 2 also). The photocatalytic activity was several times higher than that of commercial standard titania powder P25.

4. Conclusions

Base on the above experimental results, the following conclusions might be drawn:

(1) Anion doped or co-doped titania photocatalyst $TiO_{2-x}A_y$ (A = N, S) with various morphology and phase composition can be successfully prepared by mixing aqueous $TiCl_3$ solutions with various nitrogen sources at 190 °C. The $TiO_{2-x}A_y$ (A = N, S) powders showed excellent visible-light absorption and photocatalytic ability for the oxidative destruction of nitrogen monoxide under irradiation of visible light.
(2) The titania powders prepared using urea as precipitate possessed excellent visible absorption, high nitrogen doped amount and good photocatalytic activity.
(3) Nearly 25 and 86% of nitrogen monoxide could be continuously destructed under visible light ($Vis_{>500}$) and UV–vis light irradiation ($UV–vis_{>290}$). The $TiO_{2-x}N_y$ powders possessed excellent thermal stability on visible-light responsive photocatalytic activity.

Acknowledgements

This research was partially supported by the Ministry of Education, Culture, Sports, Science and Technology, a Grant-in-Aid for the COE project (Giant Molecules and Complex Systems) and a Grant-in-Aid for Science Research (No. 14750660), the Steel Industry Foundation for the Advancement of Environmental Protection Technology and the JFE 21th Century Foundation.

References

[1] R. Asahi, T. Morikawa, T. Ohwaki, K. Aoki, Y. Taga, Science 293 (2001) 269–271.
[2] T. Morikawa, R. Asahi, T. Ohwaki, K. Aoki, Y. Taga, Jpn. J. Apply. Phys. 40 (2001) L561–L563.
[3] H. Irie, Y. Watanabe, K. Hashimoto, J. Phys. Chem. B 107 (2003) 5483–5486.
[4] H. Irie, Y. Watanabe, K. Hashimoto, Chem. Lett. 32 (2003) 772–773.
[5] S.U.M. Khan, M. Al-Shahry, W.B. Ingler Jr., Science 297 (2002) 2243–2245.
[6] T. Umebayashi, T. Yamaki, S. Tanaka, K. Asai, Chem. Lett. 32 (2003) 330–331.
[7] T. Umebayashi, T. Yamaki, H. Itoh, K. Asai, Appl. Phys. Lett. 81 (2002) 454–456.
[8] I. Justicia, P. Ordejon, G. Canto, Adv. Mater. 14 (2002) 1399–1402.
[9] S. Yin, Q. Zhang, F. Saito, T. Sato, Chem. Lett. 32 (2003) 358–359.
[10] S. Yin, H. Yamaki, M. Komatsu, Q. Zhang, J. Wang, Q. Tang, F. Saito, T. Sato, J. Mater. Chem. 13 (2003) 2996–3001.
[11] J. Wang, S. Yin, Q. Zhang, F. Saito, T. Sato, J. Mater. Chem. 13 (2003) 2348–2352.
[12] Q. Zhang, J. Wang, S. YIN, T. Sato, F. Saito, J. Am. Ceram. Soc. 87 (2004) 1161–1163.
[13] S. Yin, H. Hasegawa, D. Maeda, M. Ishitsuka, T. Sato, J. Photochem. Photobiol. A 163 (2004) 1–8.
[14] N. Blazevic, D. Kolbah, B. Belin, V. Sunjic, F. Kajfez, Synthesis-Stuttgart 3 (1979) 161–176.
[15] J.M. Dreyfors, S.B. Jones, Y. Sayed, Am. Ind. Hyg. Assoc. J. 50 (1989) 579–585.
[16] W.H.R. Shaw, D.G. Walker, J. Am. Chem. Soc. 78 (1956) 5769–5772.
[17] L. Stradella, M. Argentero, Thermochim. Acta 219 (1993) 315–323.
[18] T. Ohno, T. Mitsui, M. Matusmura, Chem. Lett. 32 (2003) 364–365.
[19] Y. Aita, M. Komatsu, S. Yin, T. Sato, J. Solid State Chem. 177 (2004) 3235–3238.
[20] H. Noda, K. Oikawa, T. Ogata, K. Matsuki, H. Kamada, Chem. Soc. Jpn. 1986 (8) (1986) 1084–1090.
[21] Japanese Industrial Standard (JIS R 1701-1:2004(J)), Test method for air purification performance of photocatalytic materials. Part 1. Removal of Nitric Oxide, Japanese Standards Association, Established on 2004-01-20.
[22] H. Gerischer, A. Heller, J. Phys. Chem. 95 (1991) 5261–5267.
[23] S. Yin, T. Sato, Ind. Eng. Chem. Res. 39 (2000) 4526–4530.
[24] M. Anpo, Recent Development on Visible Light Response Type Photocatalyst, NTS, Tokyo, 2002, p. 9, ISBN 4-86043-009-03.
[25] S. Yin, Y. Inoue, S. Uchida, Y. Fujishiro, T. Sato, J. Mater. Res. 13 (1998) 844–847.
[26] S. Yin, S. Uchida, Y. Fujishiro, M. Aki, T. Sato, J. Mater. Chem. 9 (1999) 1191–1195.
[27] S. Yin, J. Wu, M. Aki, T. Sato, Inter. J. Inorg. Mater. 2 (2000) 325–331.